



ARL-TR-8243 • DEC 2017



# Energy on Target Analysis for Laser Designators

by Neal Bambha and Dan Beekman

Approved for public release; distribution is unlimited.

## **NOTICES**

### **Disclaimers**

The findings in this report are not to be construed as an official Department of the Army position unless so designated by other authorized documents.

Citation of manufacturer's or trade names does not constitute an official endorsement or approval of the use thereof.

Destroy this report when it is no longer needed. Do not return it to the originator.



# Energy on Target Analysis for Laser Designators

by Neal Bambha and Dan Beekman

*Sensors and Electron Devices Directorate, ARL*

<b>REPORT DOCUMENTATION PAGE</b>				<i>Form Approved OMB No. 0704-0188</i>	
<p>Public reporting burden for this collection of information is estimated to average 1 hour per response, including the time for reviewing instructions, searching existing data sources, gathering and maintaining the data needed, and completing and reviewing the collection information. Send comments regarding this burden estimate or any other aspect of this collection of information, including suggestions for reducing the burden, to Department of Defense, Washington Headquarters Services, Directorate for Information Operations and Reports (0704-0188), 1215 Jefferson Davis Highway, Suite 1204, Arlington, VA 22202-4302. Respondents should be aware that notwithstanding any other provision of law, no person shall be subject to any penalty for failing to comply with a collection of information if it does not display a currently valid OMB control number.</p>					
<b>PLEASE DO NOT RETURN YOUR FORM TO THE ABOVE ADDRESS.</b>					
<b>1. REPORT DATE (DD-MM-YYYY)</b> December 2017	<b>2. REPORT TYPE</b> Technical Report	<b>3. DATES COVERED (From - To)</b> 10/11/2017–12/7/2017			
<b>4. TITLE AND SUBTITLE</b> Energy on Target Analysis for Laser Designators			<b>5a. CONTRACT NUMBER</b>		
			<b>5b. GRANT NUMBER</b>		
			<b>5c. PROGRAM ELEMENT NUMBER</b>		
<b>6. AUTHOR(S)</b> Neal Bambha and Dan Beekman			<b>5d. PROJECT NUMBER</b>		
			<b>5e. TASK NUMBER</b>		
			<b>5f. WORK UNIT NUMBER</b>		
<b>7. PERFORMING ORGANIZATION NAME(S) AND ADDRESS(ES)</b> US Army Research Laboratory ATTN: RDRL-SEE-L 2800 Powder Mill Road, Adelphi, MD 20783-1138			<b>8. PERFORMING ORGANIZATION REPORT NUMBER</b> ARL-TR-8243		
<b>9. SPONSORING/MONITORING AGENCY NAME(S) AND ADDRESS(ES)</b>			<b>10. SPONSOR/MONITOR'S ACRONYM(S)</b>		
			<b>11. SPONSOR/MONITOR'S REPORT NUMBER(S)</b>		
<b>12. DISTRIBUTION/AVAILABILITY STATEMENT</b> Approved for public release; distribution is unlimited.					
<b>13. SUPPLEMENTARY NOTES</b>					
<b>14. ABSTRACT</b> One necessary condition for a successful target engagement using a laser-designated weapon system is to keep most of the laser energy on the target for most of the engagement time. This report determines the maximum range at which that is possible, given the characteristics of the target and the laser designator system.					
<b>15. SUBJECT TERMS</b> laser designator, energy on target, numerical integration, curve fitting, NATO STANAG 3733					
<b>16. SECURITY CLASSIFICATION OF:</b>		<b>17. LIMITATION OF ABSTRACT</b> UU	<b>18. NUMBER OF PAGES</b> 26	<b>19a. NAME OF RESPONSIBLE PERSON</b> Neal Bambha	
<b>a. REPORT</b> Unclassified	<b>b. ABSTRACT</b> Unclassified			<b>19b. TELEPHONE NUMBER (Include area code)</b> 301-394-5270	

## Contents

---

---

<b>List of Figures</b>	<b>iv</b>
<b>List of Tables</b>	<b>iv</b>
<b>1. Summary</b>	<b>1</b>
<b>2. Introduction</b>	<b>1</b>
<b>3. Methods, Assumptions, and Procedures</b>	<b>2</b>
3.1 Laser Beam Intensity and Integrated Power	2
3.2 Energy Contour	4
3.3 Beam Center Location	4
3.4 Numerical Integration	5
3.5 Curve Fitting	7
<b>4. Results and Discussion</b>	<b>7</b>
<b>5. Conclusions</b>	<b>12</b>
<b>6. References</b>	<b>13</b>
<b>Appendix. Numerical Integration Data</b>	<b>15</b>
<b>List of Symbols, Abbreviations, and Acronyms</b>	<b>17</b>
<b>Distribution List</b>	<b>19</b>

---

## List of Figures

---

Fig. 1	Energy contour for $\sigma_{Dh} = 15$ mrad, $R = 4.485$ km, $f_e = 0.9$ .....	6
Fig. 2	Plot of numeric integration data for $R(\chi)/R_0$ vs. $\chi$ .....	8
Fig. 3	$R(\chi)/R_0$ vs. $\chi$ with the curve fit from Eq. 16 .....	9
Fig. 4	Range vs. $\sigma_m$ for different values of $\sigma_{Dh}$ from Eq. 17 .....	10
Fig. 5	Range vs. $\chi$ using the simplified curve fit of Eq. 19 .....	11
Fig. 6	Range vs. $\sigma_m$ using the simplified curve fit of Eq. 20.....	12

---

## List of Tables

---

Table A.1	Numerical integration data for $R(\sigma_{Dh})$ vs. $\chi$ , for 5 values of $\sigma_{Dh}$ .....	16
-----------	---	----

## 1. Summary

---

One necessary condition for a successful target engagement using a laser-designated weapon system is to keep most of the laser energy on the target for most of the engagement time. This report determines the maximum range at which that is possible, given the characteristics of the target and the laser designator system.

## 2. Introduction

---

The US Army is leading the development of lightweight laser designator systems. The decreased weight is highly desirable for a man-portable system, but the trade-off is reduced laser output power, which leads to concern about the performance of the system when used with a variety of tri-service and coalition weapons systems.

The applicable NATO standard agreement is STANAG 3733, *Laser Pulse Repetition Frequencies Used for Target Designation and Weapon Guidance*, which is in the process of being revised. The current edition of the STANAG specifies that a compliant laser designator system has a minimum laser output energy of 50 mJ per pulse (NATO 2005).

A proposed revision of the STANAG deletes the minimum laser energy specification and instead describes a modeling and simulation approach to determine the range at which a laser designator system will function successfully with a certain weapon system. The modeling and simulation is performed in 2 phases: energy on target (EoT) and weapon system performance.

The EoT phase is designed to ensure that most of the laser energy stays on the target most of the time to avoid “overspill”, or laser energy missing the target and reflecting from the background, which could cause a weapon to miss the target. A standard NATO target is 2.3 by 2.3 m for a vehicle-sized target, and the proposed EoT metric is 90% of the laser energy on the target 95% of the engagement time. For generality, we denote the fraction of laser energy on target as  $f_e$  and the fraction of beam center locations that result in  $f_e$  as  $f_c$ .

This report will address only the EoT phase, not the more complicated weapon system performance phase, and the analysis presented here is sufficiently general to apply to any laser designator system.

### 3. Methods, Assumptions, and Procedures

---

The EoT problem is to determine the maximum range at which the EoT metric can be met for a specified laser designator. This requires calculation of both the laser beam size and the distribution of possible locations for the beam center on the target.

The laser beam size is defined by the beam waist or beam divergence, and the laser beam intensity distribution is assumed to be Gaussian. Beam center location can be affected by boresight error, platform jitter, atmospheric turbulence, or other factors, which will be collectively referred to as motion. We will assume that these factors are random and independently varying, and that the motion statistics can also be described by a Gaussian distribution with a mean equal to zero.

Our approach to the EoT problem is to numerically integrate the total laser energy over the area of the standard NATO target for all locations of the laser beam center on the target, given the range, beam divergence, and motion standard deviation. A binary search is conducted on the range to determine the maximum range for  $f_e$  energy on target for  $f_c$  of the time. The resulting data can then be described by an equation that is determined to provide the best fit.

#### 3.1 Laser Beam Intensity and Integrated Power

---

Laser beam spot size is specified by the beam waist radius,  $w_R$ , measured from the beam central axis to the point at which the intensity falls to  $1/e^2$  of the center intensity, at a specified range,  $R$ . The beam waist increases linearly with range, so the spot size radius can also be specified by the beam divergence (half-angle),  $\sigma_{Dh} = w_R/R$  in milliradians if  $w_R$  is in meters and  $R$  is in kilometers.

The Gaussian beam intensity distribution  $I(x, y, x_c, y_c, w_R)$  is given by

$$I(x, y, x_c, y_c, w_R) = \frac{2P_{\text{total}}}{\pi w_R^2} e^{-2[(x-x_c)^2 + (y-y_c)^2]/w_R^2}, \quad (1)$$

where  $P_{\text{total}}$  is the total power in the beam, and  $(x_c, y_c)$  is the location of the beam center. The integrated power over the target is

$$P(x_c, y_c, w_R, L) = \frac{4 \cdot 2P_{\text{total}}}{\pi w_R^2} \iint_0^{L/2} e^{\frac{-2[(x-x_c)^2 + (y-y_c)^2]}{w_R^2}} dx dy,$$

where  $L$  is the length of a side of the square NATO target. By integrating the power over the duration of a single laser pulse, we obtain an equivalent equation for the laser energy per pulse on the target,  $E(w_R, L)$ :

$$E(x_c, y_c, w_R, L) = \frac{4 \cdot 2E_{total}}{\pi w_R^2} \iint_0^{L/2} e^{\frac{-2[(x-x_c)^2+(y-y_c)^2]}{w_R^2}} dx dy. \quad (2)$$

With the beam centered on the target ( $x_c = y_c = 0$ ), the maximum range for  $f_e$  energy on target,  $R_0(f_e)$ , can be calculated from Eq. 2 by

$$\frac{E(w, L)}{E_{total}} = \frac{4 \cdot 2}{\pi w_R^2} \iint_0^{L/2} e^{\frac{-2(x^2+y^2)}{w_R^2}} dx dy = \frac{8}{\pi w_R^2} \left[ \int_0^{L/2} e^{\frac{-2(x^2)}{w_R^2}} dx \right]^2 = f_e .$$

This can be rewritten in the form of the error function, erf:

$$\text{erf}(x) = \frac{2}{\sqrt{\pi}} \int_0^x e^{-u^2} du$$

by using a substitution of variables,

$$u = \frac{\sqrt{2}x}{w_R}, \quad \text{so } \frac{w_R}{\sqrt{2}} du = dx,$$

and for the limit of integration,

$$\text{when } x = \frac{L}{2}, \text{ then } u = \frac{L}{\sqrt{2}w_R} .$$

The resulting equation for fractional energy on target is

$$\frac{E(w_R, L)}{E_{total}} = \frac{8}{\pi w_R^2} \cdot \left[ \left( \frac{w_R}{\sqrt{2}} \cdot \frac{\sqrt{\pi}}{2} \right) \cdot \frac{2}{\sqrt{\pi}} \int_0^{\frac{L}{\sqrt{2}w_R}} e^{-u^2} du \right]^2 = \left[ \text{erf} \left( \frac{L}{\sqrt{2}w_R} \right) \right]^2 = f_e .$$

We can obtain the argument of the error function by using the inverse error function, erfinv, which is a callable function in many numerical analysis software packages such as MATLAB:

$$\frac{L}{\sqrt{2}w_R} = \text{erfinv}(\sqrt{f_e}), \text{ so } w_R = \sigma_{Dh} R_0(f_e) = \frac{L}{\sqrt{2} \text{erfinv}(\sqrt{f_e})} . \quad (3)$$

For  $f_e = 0.9$ , as in NATO STANAG 3733,

$$R_0(0.9) = \frac{L}{1.95\sigma_{Dh}}. \quad (4)$$

### 3.2 Energy Contour

---

For a beam that is centered at location  $(x_c, y_c)$ , the energy on target can be obtained by Eq. 2. We then define an energy contour function  $K(x_c, y_c, w_R, f_e)$  or  $K(x_c, y_c, \sigma_{Dh}, R, f_e)$ , which characterizes each point on the target as to whether a beam centered at that point meets the specification for  $f_e$ :

$$K(x_c, y_c, \sigma_{Dh}, R, f_e) = \begin{cases} 1, & \frac{E(x_c, y_c)}{E_t} \geq f_e \\ 0, & \frac{E(x_c, y_c)}{E_t} < f_e \end{cases}. \quad (5)$$

### 3.3 Beam Center Location

---

The probability distribution of the beam center location is given by the motion statistics

$$M(x, y, \sigma_m, R) = \frac{1}{2\pi\sigma_m^2 R^2} e^{-\frac{(x^2+y^2)}{2\sigma_m^2 R^2}}, \quad (6)$$

where  $\sigma_m$  is the motion standard deviation and  $R$  is the range.

The probability,  $\Pi$ , of the beam meeting the specification for  $f_e$  can be calculated by integrating the probability distribution  $M$  over points for which  $f_e$  meets the specification

$$\Pi(R, \sigma_m, \sigma_{Dh}, f_e) = \iint_{-L/2}^{L/2} M(x, y, \sigma_m, R) K(x, y, \sigma_{Dh}, R, f_e) dx dy. \quad (7)$$

Therefore, for a given  $\sigma_m, \sigma_{Dh}$ , and  $f_e$ , it is necessary to find the range  $R$  that satisfies the specification for  $f_c$ . Here, we used a binary search algorithm to determine the range for which

$$\Pi(R, \sigma_m, \sigma_{Dh}, f_e) = f_c. \quad (8)$$

It is instructive to investigate the case where  $\sigma_m \gg \sigma_{Dh}$ . In this case we can approximate  $K(x, y, \sigma_{Dh}, R, f_e) \approx 1$ . Then Eq. 7 becomes

$$\Pi(R, \sigma_m \gg \sigma_{Dh}) \approx \frac{4}{2\pi\sigma_m^2 R^2} \iint_0^{L/2} e^{-\frac{(x^2+y^2)}{2\sigma_m^2 R^2}} dx dy. \quad (9)$$

The integral can be determined as it is for Eq. 2, using the variable substitution

$$u = \frac{x}{\sqrt{2}\sigma_m R}, \quad \text{so } \sqrt{2}\sigma_m R du = dx$$

and for the limit of integration

$$\begin{aligned} \text{when } x = \frac{L}{2}, \text{ then } u &= \frac{L}{2\sqrt{2}\sigma_m R} \\ \Pi(R, \sigma_m \gg \sigma_{Dh}) &= \frac{4}{2\pi\sigma_m^2 R^2} \cdot \left[ \left( \sqrt{2}\sigma_m R \cdot \frac{\sqrt{\pi}}{2} \right) \cdot \frac{2}{\sqrt{\pi}} \int_0^{\frac{L}{2\sqrt{2}\sigma_m R}} e^{-u^2} du \right]^2 \\ &= \left[ \operatorname{erf} \left( \frac{L}{2\sqrt{2}\sigma_m R} \right) \right]^2 = f_c \\ \frac{L}{2\sqrt{2}\sigma_m R} &= \operatorname{erfinv}(\sqrt{f_c}) \\ \sigma_m R(f_c) &= \frac{L}{2\sqrt{2}\operatorname{erfinv}(\sqrt{f_c})}. \end{aligned} \quad (10)$$

For  $f_c = 0.95$ , as in NATO STANAG 3733,

$$\sigma_m R(f_c) = \frac{L}{4.473}. \quad (11)$$

### 3.4 Numerical Integration

---

The numerical integration of laser energy on the standard NATO target board was initiated by setting up a 2-D grid of  $231 \times 231$  elements on the 2.3- by 2.3-m target board. This gave a total of 53361 elements.

The energy on target is calculated by choosing a value for the laser beam divergence in milliradians (mrad), then choosing an initial range in kilometers, then positioning the beam center at each point on the grid. For each beam center location, the energy at each element on the target board is calculated using Eq. 2. The values at all elements are totaled to determine the fraction of laser energy on the target board. If the energy on target is less than  $f_e$ , the beam center location is given a weighting factor of zero, as expressed in Eq. 5 for the energy contour. If the energy on target

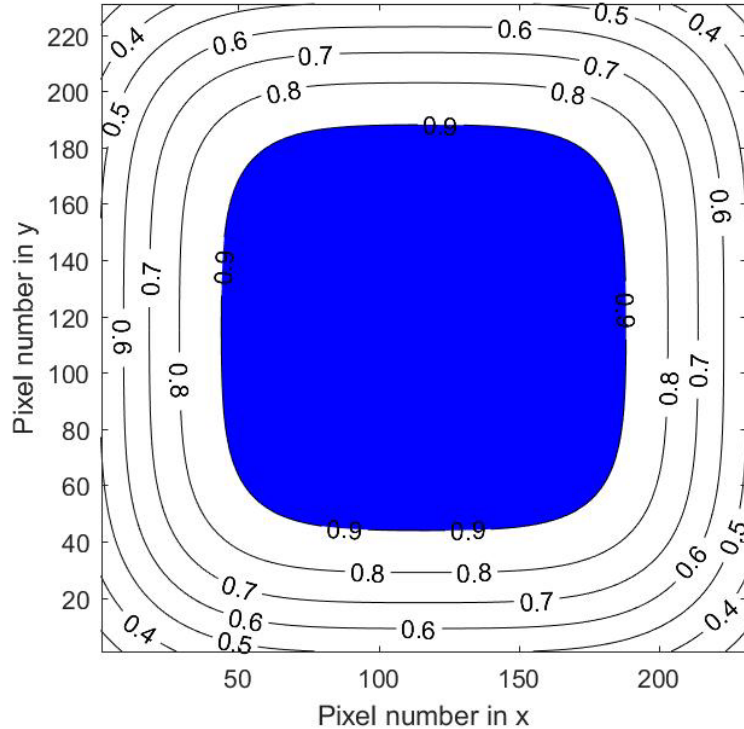
is  $f_e$  or greater, the location is given a weighting factor calculated by Eq. 6, using the specified value for the motion standard deviation. This weighting factor is the relative frequency of occurrence for this beam location in the total beam center distribution. All weighting factors for all beam locations are totaled to determine the fraction,  $\Pi$ , of the motion distribution that resulted in  $f_e$  energy on target. This is expressed in Eq. 7, in which it can be seen that  $\Pi$  is a function of the range. A binary search routine is used to determine the range at which  $\Pi = f_c$  (i.e., where  $f_c$  of the beam center distribution results in  $f_e$  energy on target [Eq. 8]).

Figure 1 shows the energy contour ( $x_c, y_c, \sigma_{Dh} = 0.15$  mrad,  $R = 4.485$  km,  $f_e = 0.9$ ). Here, the range  $R = 4.485$  km resulted from a binary search with  $\sigma_m = 0.07$  mrad and  $f_c = 0.95$ . The center section in blue corresponds to the beam center locations  $(x_c, y_c)$  for which  $E(x_c, y_c)/E_t > 0.9$ .

For our data set, we used  $\sigma_{Dh} = 0.05, 0.075, 0.1, 0.15$ , and  $0.2$  mrad. For each value of  $\sigma_{Dh}$ , the range was calculated for values of  $\sigma_m$  from  $0$  to  $0.3$  mrad in increments of  $0.01$  mrad. Therefore,  $\chi = \sigma_m/\sigma_{Dh}$  varies from  $0$  to  $6$ .

We used the NATO STANAG 3733 criteria to set  $f_e = 0.9$  and  $f_c = 0.95$ .

The data are plotted in Section 4, with the numeric values tabulated in the Appendix.



**Fig. 1 Energy contour for  $\sigma_{Dh} = 15$  mrad,  $R = 4.485$  km,  $f_e = 0.9$**

### 3.5 Curve Fitting

---

The first step in curve fitting is to choose an equation that fits the general shape of the data. Coefficients can then be determined by first considering extreme values, then by using standard curve-fitting routines.

Based on the data shown in Fig. 2, our choice for the equation to fit the data is of the form

$$R(\chi) = R_0 \frac{A\chi + B}{\chi^2 + C\chi + B}, \quad (12)$$

where  $= \sigma_m / \sigma_{Dh}$ .

When  $\chi = 0$ , then  $R(\chi) = R_0$ , which was calculated in Eq. 3.

When  $\chi \gg 1$  (i.e.,  $\sigma_m \gg \sigma_{Dh}$ ), we have

$$R(\chi)\sigma_m = R_0 \frac{A\chi + B}{\chi^2 + C\chi + B} \sigma_m \rightarrow R_0 \frac{A}{\chi} \sigma_m. \quad (13)$$

Comparing Eqs. 13 and 10, and using Eq. 3 for  $R_0$ ,

$$\begin{aligned} R(\chi)\sigma_m \rightarrow R_0 \cdot \frac{A}{\chi} \sigma_m &= \frac{L}{\sigma_{Dh} \sqrt{2} \operatorname{erfinv}(\sqrt{f_e})} \frac{A}{\chi} \sigma_m = \frac{L}{2\sqrt{2} \operatorname{erfinv}(\sqrt{f_c})} \\ \frac{L}{\sigma_{Dh}} \frac{A}{(\sigma_m / \sigma_{Dh})} \sigma_m &= \frac{L \sqrt{2} \operatorname{erfinv}(\sqrt{f_e})}{2\sqrt{2} \operatorname{erfinv}(\sqrt{f_c})} \\ A &= \frac{\operatorname{erfinv}(\sqrt{f_e})}{2 \operatorname{erfinv}(\sqrt{f_c})}. \end{aligned} \quad (14)$$

So we can substitute this value for  $A$  and our fitting equation becomes

$$R(\chi) = R_0 \frac{\left( \frac{\operatorname{erfinv}(\sqrt{f_e})}{2 \operatorname{erfinv}(\sqrt{f_c})} \right) \chi + B}{\chi^2 + C\chi + B}. \quad (15)$$

## 4. Results and Discussion

---

An interesting feature of the data is to note that a plot of  $R(\chi)/R_0$  versus  $\chi$  results in all the data falling along a single curve for all values of  $\sigma_{Dh}$ , as seen in Fig. 2.

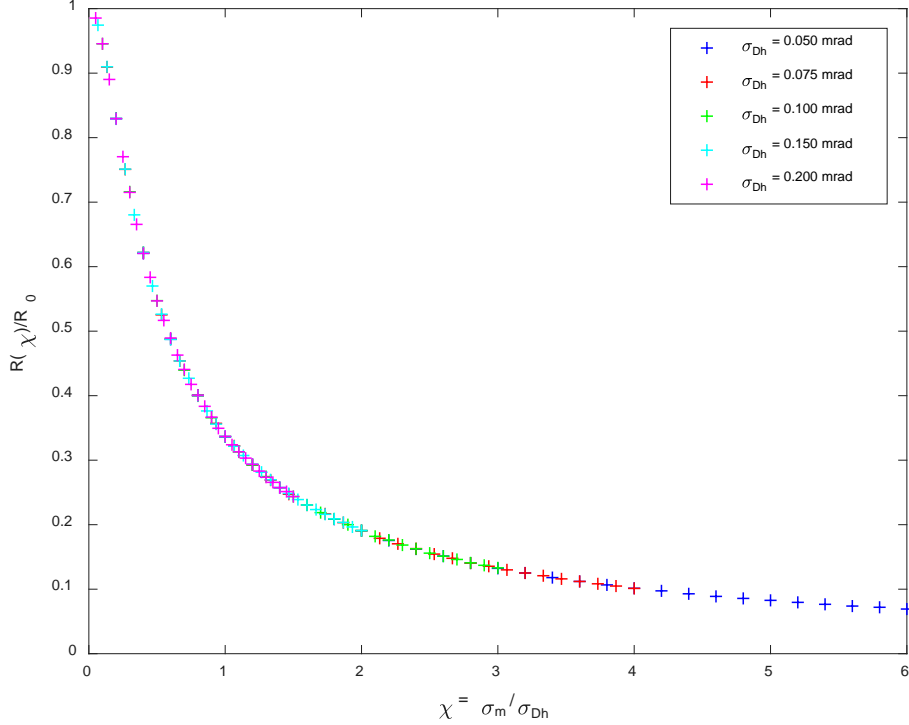


**Fig. 2** Plot of numeric integration data for  $R(\chi)/R_0$  vs.  $\chi$

This indicates that the function is characteristic of the square target and the parameters  $f_e$  and  $f_c$ .

We can use Eq. 15 as the fitting equation, and substituting in Eq. 14 for  $f_e$  and  $f_c$ , the coefficient  $A = 0.436$ . Using a fitting routine, the other coefficients are found to be  $B = 0.0582$  and  $C = 0.391$ . The final fitting equation is

$$R(\chi) = R_0 \frac{0.436\chi + 0.0582}{\chi^2 + 0.391\chi + 0.0582} \quad (16)$$

with  $R_0$  given by Eq. 4. The results are shown in Fig. 3. The fit of Eq. 16 to the data is excellent for all values of  $\sigma_{Dh}$  and  $\chi$ .

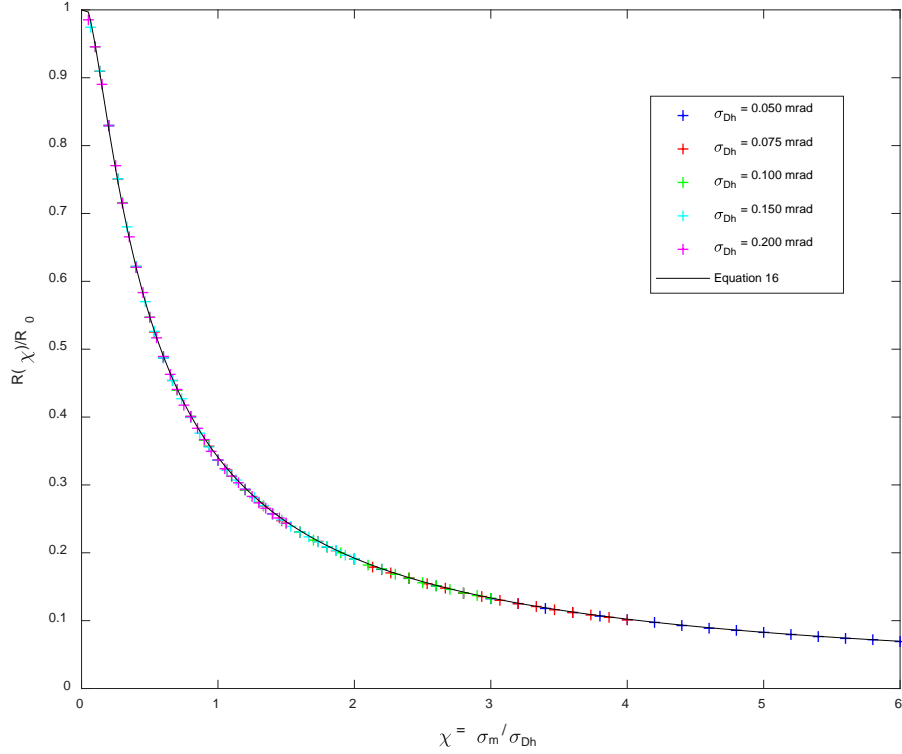


**Fig. 3**  $R(\chi)/R_0$  vs.  $\chi$  with the curve fit from Eq. 16

We can rewrite Eq. 16 in terms of the basic input parameters  $L$ ,  $\sigma_m$ , and  $\sigma_{Dh}$  by substituting  $\chi = \sigma_m/\sigma_{Dh}$  and  $R_0 = L/1.95\sigma_{Dh}$ :

$$R(L, \sigma_m, \sigma_{Dh}) = L \frac{0.223\sigma_m + 0.030\sigma_{Dh}}{\sigma_m^2 + 0.391\sigma_m\sigma_{Dh} + 0.058\sigma_{Dh}^2}. \quad (17)$$

Figure 4 shows the numeric integration results and Eq. 17 for range with each value of  $\sigma_{Dh}$  on a separate curve.

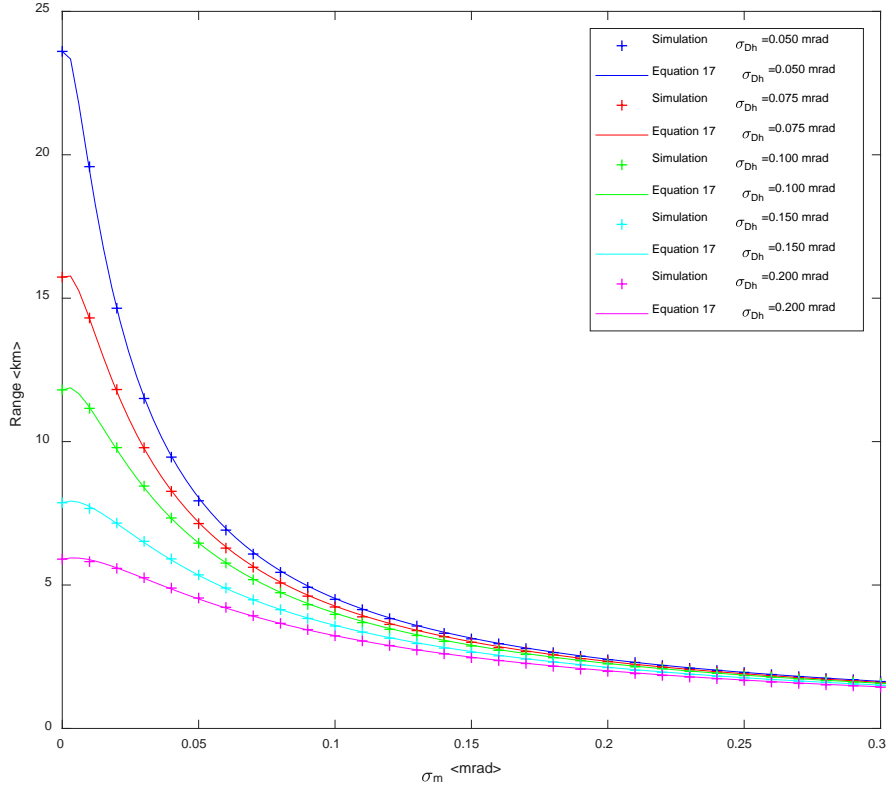


**Fig. 4 Range vs.  $\sigma_m$  for different values of  $\sigma_{Dh}$  from Eq. 17**

The fit of Eq. 17 to the data is excellent for all values of  $\sigma_m$  and  $\sigma_{Dh}$ .

For application of this analysis in the field, it has been suggested that a simpler equation would be much preferred. It can also be argued that, in practice, the value of  $\chi$  will almost always be greater than 0.2. Therefore, we look again at Eq. 16 with the goal to simplify without giving up significant accuracy for  $\chi > 0.2$ .

It can be seen that the coefficient B in Eq. 15 turns out to be small in Eq. 16, so we set B = 0 to simplify the equation. Equation 16 then becomes

$$R(\chi) = R_0 \frac{0.436\chi + 0}{\chi^2 + C\chi + 0} = R_0 \frac{0.436}{\chi + C}. \quad (18)$$

Again using a fitting routine using only data with  $\chi > 0.2$ , the coefficient C is now determined to be 0.306, so the new, simplified fitting equation is

$$R(\chi) = R_0 \frac{0.436}{\chi + 0.306}. \quad (19)$$

The results of using the simplified fitting equation are shown in Fig. 5.

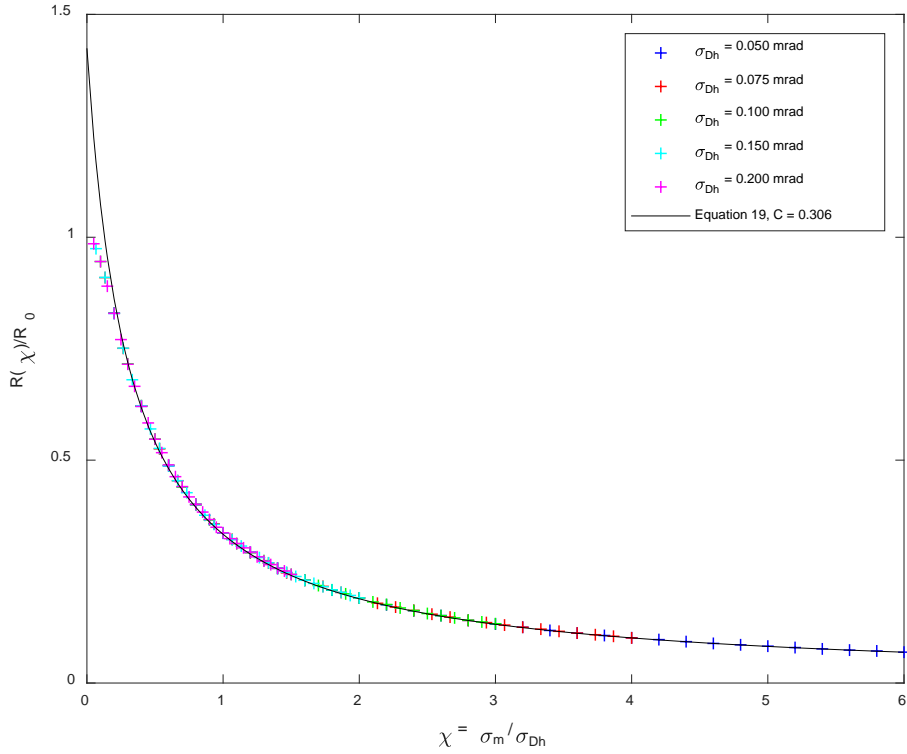


**Fig. 5** Range vs.  $\chi$  using the simplified curve fit of Eq. 19

It can be seen that the fit to the data is not as good for small values of  $\chi$  but is reasonably close for  $\chi > 0.2$ .

We will now rewrite Eq. 19 in terms of the basic input parameters  $L$ ,  $\sigma_m$ , and  $\sigma_{Dh}$ , using Eq. 4 for  $R_0$  and the previous definition  $\chi = \sigma_m/\sigma_{Dh}$ :

$$R(\chi) = R_0 \frac{0.436}{\chi + 0.306} = \frac{L}{1.95\sigma_{Dh}} \left[ \frac{0.436}{(\sigma_m/\sigma_{Dh}) + 0.306} \right]$$

$$R(L, \sigma_m, \sigma_{Dh}) = \frac{L}{4.47\sigma_m + 1.37\sigma_{Dh}}. \quad (20)$$

Equation 20 is similar to the equation that has been recently proposed for use in NATO STANAG 3733 based on a separate analysis (Robertson 2017), with the difference being the coefficient 1.37 determined here is replaced by a value of 2.0.

The fit of Eq. 20 to the data for  $R$  versus  $\sigma_m$  is shown in Fig. 6.

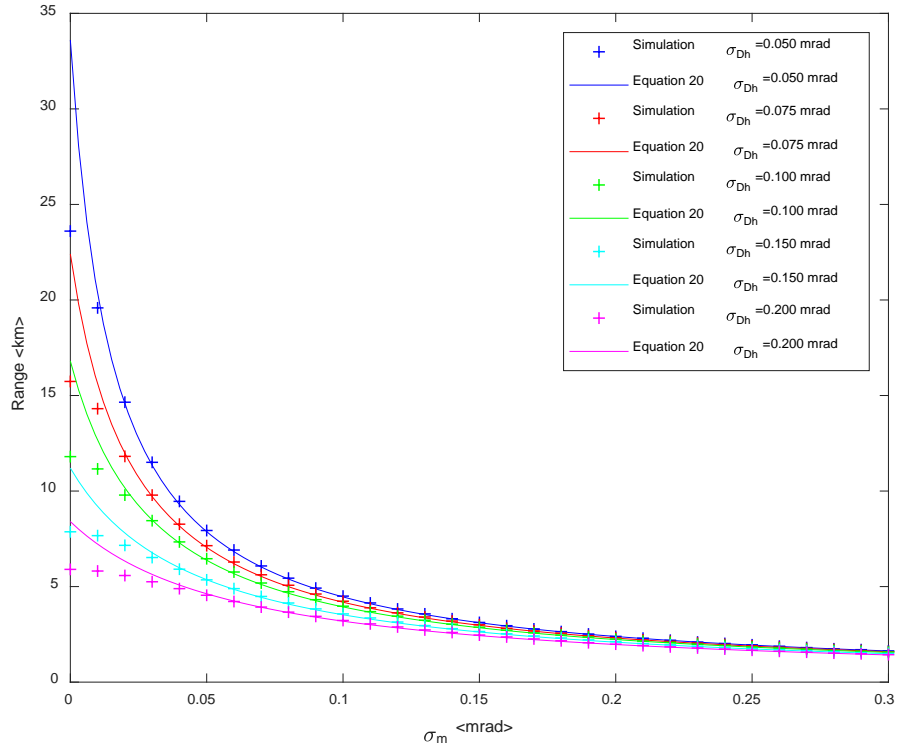


**Fig. 6 Range vs.  $\sigma_m$  using the simplified curve fit of Eq. 20**

## 5. Conclusions

To address the modeling and simulation process called for in the draft revision to NATO STANAG 3733 regarding laser designators, we performed an Energy on Target analysis using numerical integration, and we used curve fitting to identify an equation that accurately represents the data. We also identified a simpler version of the equation that fits the data well for practical parameter values. This analysis will help the Soldier determine the appropriate range for successful application of laser designators in the field.

## **6. References**

---

NATO STANAG 3733. Laser pulse repetition frequencies used for target designation and weapon guidance. n.p.: North Atlantic Treaty Organization; 2005 Apr.

Robertson M. Huntsville (AL): Gleason Research Associates; unpublished briefing to the Laser Designator Working Group, 2017 Oct.

INTENTIONALLY LEFT BLANK.

## **Appendix. Numerical Integration Data**

---

**Table A.1 Numerical integration data for  $R(\sigma_{Dh})$  vs.  $\chi$ , for 5 values of  $\sigma_{Dh}$**

$\chi$	$R(.05)$	$\chi$	$R(.075)$	$\chi$	$R(.10)$	$\chi$	$R(.15)$	$\chi$	$R(.20)$
0.00	1.0000	0.00	1.0000	0.00	1.0000	0.00	1.0000	0.00	1.0000
0.20	0.8298	0.13	0.9095	0.10	0.9455	0.07	0.9744	0.05	0.9854
0.40	0.6206	0.27	0.7509	0.20	0.8295	0.13	0.9099	0.10	0.9456
0.60	0.4874	0.40	0.6220	0.30	0.7160	0.20	0.8289	0.15	0.8902
0.80	0.4008	0.53	0.5253	0.40	0.6218	0.27	0.7512	0.20	0.8292
1.00	0.3362	0.67	0.4539	0.50	0.5473	0.33	0.6803	0.25	0.7704
1.20	0.2929	0.80	0.3995	0.60	0.4884	0.40	0.6221	0.30	0.7152
1.40	0.2576	0.93	0.3570	0.70	0.4396	0.47	0.5700	0.35	0.6656
1.60	0.2305	1.07	0.3222	0.80	0.4009	0.53	0.5263	0.40	0.6206
1.80	0.2085	1.20	0.2930	0.90	0.3658	0.60	0.4873	0.45	0.5834
2.00	0.1907	1.33	0.2691	1.00	0.3368	0.67	0.4538	0.50	0.5469
2.20	0.1755	1.47	0.2472	1.10	0.3126	0.73	0.4270	0.55	0.5167
2.40	0.1622	1.60	0.2305	1.20	0.2927	0.80	0.3998	0.60	0.4893
2.60	0.1513	1.73	0.2168	1.30	0.2746	0.87	0.3763	0.65	0.4629
2.80	0.1405	1.87	0.2032	1.40	0.2572	0.93	0.3559	0.70	0.4407
3.00	0.1323	2.00	0.1908	1.50	0.2436	1.00	0.3368	0.75	0.4175
3.20	0.1251	2.13	0.1789	1.60	0.2305	1.07	0.3216	0.80	0.4008
3.40	0.1180	2.27	0.1704	1.70	0.2187	1.13	0.3072	0.85	0.3835
3.60	0.1120	2.40	0.1629	1.80	0.2089	1.20	0.2939	0.90	0.3668
3.80	0.1067	2.53	0.1544	1.90	0.2000	1.27	0.2813	0.95	0.3494
4.00	0.1014	2.67	0.1479	2.00	0.1908	1.33	0.2696	1.00	0.3369
4.20	0.0974	2.80	0.1404	2.10	0.1819	1.40	0.2571	1.05	0.3239
4.40	0.0929	2.93	0.1356	2.20	0.1762	1.47	0.2483	1.10	0.3130
4.60	0.0888	3.07	0.1300	2.30	0.1684	1.53	0.2389	1.15	0.3032
4.80	0.0857	3.20	0.1251	2.40	0.1627	1.60	0.2305	1.20	0.2936
5.00	0.0827	3.33	0.1209	2.50	0.1559	1.67	0.2235	1.25	0.2831
5.20	0.0796	3.47	0.1160	2.60	0.1512	1.73	0.2161	1.30	0.2735
5.40	0.0766	3.60	0.1120	2.70	0.1461	1.80	0.2090	1.35	0.2656
5.60	0.0738	3.73	0.1084	2.80	0.1408	1.87	0.2035	1.40	0.2572
5.80	0.0720	3.87	0.1049	2.90	0.1370	1.93	0.1965	1.45	0.2513
6.00	0.0692	4.00	0.1012	3.00	0.1331	2.00	0.1909	1.50	0.2436

Note: See Section 3.4 for numerical integration procedure and other parameter values.

## List of Symbols, Abbreviations, and Acronyms

---

A	coefficient in the curve-fit equation
B	coefficient in the curve-fit equation
C	coefficient in the curve-fit equation
E	energy in a single laser pulse
erf	error function
erfinv	inverse error function
$f_e$	fraction of laser energy on target
$f_c$	fraction of laser beam center locations that result in $f_e$
I	laser beam intensity distribution
K	contour function
L	length of a side of a square NATO target
M	probability distribution for the laser beam center location
P	power in the laser beam
$\Pi$	integrated probability distribution for the laser beam center location
R	range from laser designator to target
$R_0$	maximum range for $f_e$ energy on target with the laser beam centered on the center of the target
u	generic integration variable
x	horizontal dimension of the target
y	vertical dimension of the target
$x_c$	horizontal location of the laser beam center on the target
$y_c$	vertical location of the laser beam center on the target
$w_R$	laser beam waist radius
$\chi$	ratio of motion standard deviation to divergence half-angle
$\sigma_{Dh}$	divergence half-angle

$\sigma_m$	motion standard deviation for location of the laser beam center
2-D	2-dimensional
ARL	US Army Research Laboratory
EoT	Energy on Target
NATO	North Atlantic Treaty Organization
STANAG	Standard Agreement (NATO)

1 DEFENSE TECHNICAL  
(PDF) INFORMATION CTR  
DTIC OCA

2 DIR ARL  
(PDF) IMAL HRA  
RECORDS MGMT  
RDRL DCL  
TECH LIB

1 GOVT PRINTG OFC  
(PDF) A MALHOTRA

2 ARL  
(PDF) RDRL SE  
D BEEKMAN  
RDRL SEE L  
N BAMBHA

INTENTIONALLY LEFT BLANK.